DOI: 10.1534/genetics.110.118802

A Genomic Imprinting Defect in Mice Traced to a Single Gene

Altan Rentsendorj,*[,1] Subburaman Mohan,[†] Piroska Szabó*[,2] and Jeffrey R. Mann*[,‡,§,3]

**Division of Biology, Beckman Research Institute, City of Hope National Medical Center, Duarte, California 91010, [†]Musculoskeletal Diseases Center, Jerry L. Pettis Memorial Veterans Affairs Medical Center, Loma Linda, California 92357, [‡]Theme of Laboratory and Community Genetics, Murdoch Children's Research Institute, The Royal Children's Hospital, Parkville 3052, Victoria, Australia and [§]Department of Zoology, The University of Melbourne, Melbourne 3010, Victoria, Australia*

Manuscript received May 16, 2010
Accepted for publication August 10, 2010

ABSTRACT

Mammalian androgenones have two paternally or sperm-derived genomes. In mice (*Mus musculus*) they die at peri-implantation due to the misexpression of imprinted genes—the genes that are expressed monoallelically according to the parent of origin. The misexpressions involved are poorly defined. To gain further insight, we examined the causes of midgestation death of embryos with paternal duplication (PatDp) of distal chromosome 7 (dist7), a region replete with imprinted genes. PatDp(dist7) embryos have a similar phenotype to mice with a knockout of a maternally expressed imprinted gene, *Ascl2* [*achaete-scute complex homolog-like 2* (Drosophila)], and their death at midgestation could result from two inactive paternal copies of this gene. However, other dist7 misexpressions could duplicate this phenotype, and the potential epistatic load is undefined. We show that an *Ascl2* transgene is able to promote the development of PatDp(dist7) embryos to term, providing strong evidence that *Ascl2* is the only imprinted gene in the genome for which PatDp results in early embryonic death. While some of the defects in perinatal transgenic PatDp(dist7) fetuses were consistent with known misexpressions of dist7 imprinted genes, the overall phenotype indicates a role for additional undefined misexpressions of imprinted genes. This study provides implications for the human imprinting-related fetal overgrowth disorder, Beckwith–Wiedemann syndrome.

In mice, *Mus musculus*, partheno- and androgenones, with two maternal and paternal genomes, respectively, die early at the peri-implantation stage. This developmental failure involves genomic imprinting, an epigenetic system in mammals resulting in the parent-specific monoallelic expression of a small subset of genes, many of which are crucial for normal growth and development. Parthenogenones overexpress maternally, and lack expression of paternally expressed imprinted genes, while the opposite misexpressions occur in androgenones (Barton *et al.* 1984; Mann and Lovell-Badge 1984; McGrath and Solter 1984; Surani *et al.* 1984; Cattanach and Kirk 1985; Coan *et al.* 2005; Fowden *et al.* 2006). Understanding how the various misexpressions combine to bring about the death of partheno- and androgenones is important for understanding the etiology of genomic imprinting (Solter 2006; Wood and Oakey 2006; Renfree *et al.* 2009) and the prevalence of sexual reproduction (Avise 2008).

An important region in terms of genomic imprinting is distal chromosome 7 (dist7), which contains >20 imprinted genes and at least two imprinting control regions (ICRs) (Schulz *et al.* 2006; Williamson *et al.* 2010) (Figure 1). The *Igf2/H19* (*insulin-like growth factor 2/H19 fetal liver mRNA*) ICR, or ICR1, functions as a DNA methylation-sensitive CTCF (CCCTC-binding factor)-based chromatin insulator. On the maternal chromosome, ICR1 binds CTCF and blocks *Igf2* promoter–enhancer interaction. On the paternal chromosome, ICR1 is hypermethylated, which prevents CTCF binding. *Igf2* promoter–enhancer interaction is therefore allowed (Bell and Felsenfeld 2000; Hark *et al.* 2000; Szabó *et al.* 2000). Telomeric to the ICR1 domain is a large cluster of imprinted genes under regulatory control of the KvDMR1 ICR, or ICR2. The active state of maternally derived genes within this cluster coincides with maternal-specific ICR2 hyper-methylation and the inactive state of the *Kcnq1ot1* (*KCNQ1 overlapping transcript 1*) gene promoter contained within ICR2. The paternal ICR2 is hypomethylated, and paternal-specific elongation of the *Kcnq1ot1* transcript is associated with silencing of genes within the cluster in *cis* (Fitzpatrick *et al.* 2002; Mancini-Dinardo *et al.* 2006; Shin *et al.* 2008).

Research with mice with maternal and paternal duplication (MatDp and PatDp) of chromosome regions has identified regions of the genome subject to imprinting (Williamson *et al.* 2010). Mice with MatDp

[1]*Present address*: Department of Neurosurgery, Cedars Sinai Medical Center, Los Angeles, CA 90048.

[2]*Present address*: Department of Molecular and Cellular Biology, Beckman Research Institute, City of Hope National Medical Center, Duarte, CA 91010.

[3]*Corresponding author:* Theme of Laboratory and Community Genetics, Murdoch Children's Research Institute, The Royal Children's Hospital, Flemington Rd., Parkville 3052, Victoria, Australia.
E-mail: jeff.mann@mcri.edu.au

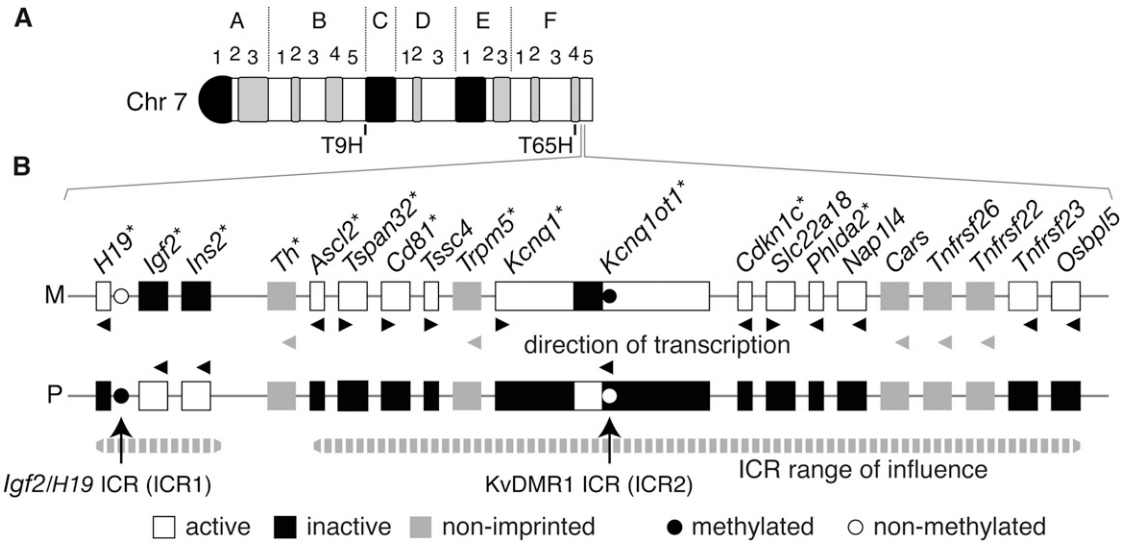

Figure 1.—Imprinted genes regulated by ICR1 and ICR2. (A) Ideogram of G-banded mouse chromosome 7. The T9H and T65H breakpoints are at the B5/C border and F4, respectively, while the imprinted genes regulated by ICR1 and ICR2 are at F4/5. (B) All known genes within the two ICR clusters, imprinted and non-imprinted, are shown. Maternal (M) and paternal (P) chromosome. Genes for which knockouts have been published are indicated with an asterisk. Adapted partly from Beechey *et al.* (1997) and Hudson *et al.* (2010).

and PatDp of dist7, as defined by the T(7;15)9H (T9H) and T(7;11)65H (T65H) reciprocal translocation breakpoints, die perinatally and early in gestation, respectively (Searle and Beechey 1990; McLaughlin *et al.* 1996; Beechey *et al.* 1997). Mice with MatDp can be rescued through introduction of a mutant ICR1, which corrects misexpressions associated with two maternally derived ICRs, with *Igf2* activation probably crucial (Han *et al.* 2010). The cause of death of PatDp(dist7) embryos is unknown. The phenotype of PatDp(dist7)T9H embryos appears identical to mice with a null mutation of the dist7 imprinted gene *Ascl2* [*achaete-scute complex homolog-like 2* (Drosophila)], encoding a transcription factor essential for proliferation of placental spongiotrophoblast (Guillemot *et al.* 1995; McLaughlin *et al.* 1996). Maternal-specific expression of this and many other genes, including *Cdkn1c* [*cyclin-dependent kinase inhibitor 1C* (P57)], is regulated by ICR2 (Fitzpatrick *et al.* 2002). While PatDp(dist7)T9H death is consistent with the presence of two paternally derived and epigenetically inactive copies of *Ascl2* (McLaughlin *et al.* 1996), other misexpressions could duplicate this phenotype. Furthermore, the epistatic load of other dist7 misexpressions is likely to be considerable. Indeed, studies of PatDp(dist7)T9H embryonic stem (ES) cell chimeras revealed a potent negative effect of these cells on fetal development, akin to chimeras produced with androgenetic ES cells. Chimeras died at the fetal stage and possessed marked overgrowth of liver and heart and abdominal and skeletal defects (McLaughlin *et al.* 1997). Dist7 is likely to be an important influence in terms of failed androgenetic development as extensive and essentially complete genome-wide analysis has revealed that this is the only PatDp resulting in death at an early embryonic stage (Cattanach and Beechey 1997; Williamson *et al.* 2010).

To better define how imprinted genes at the localized level of dist7 work together in regulating normal development, and to provide further insight into the developmental failure of androgenones, we examined some of the misexpressions of imprinted genes that might cause the developmental failure of PatDp(dist7)T9H conceptuses. We tested the developmental potential of PatDp(dist7)T9H embryos for which expression of *Ascl2* was restored through the introduction of an *Ascl2* transgene. This transgene resulted in the survival of PatDp(dist7)T9H embryos to late gestation with occasional live births. Nevertheless, defects were still observed with other misexpressions coming into play. Overexpression of *Igf2* was corrected through the introduction of an *Igf2* null mutation, which had some ameliorating effect. These findings provide implications for the human congenital imprinting-related disorder, Beckwith–Wiedemann syndrome, which is often associated with PatDp of the orthologous chromosome region.

MATERIALS AND METHODS

Mouse lines: The following indicates the line, genotype, strain, source, and how it was produced and maintained: line 1—$Tyr^{+/+}$, 129S1/SvImJ, The Jackson Laboratory (stock no. 002448); line 2—$Tyr^{c/c}$, outbred Swiss CF-1, Charles River Laboratories; line 3—T9H/T9H, $Tyr^{+/+}$, mix of C57BL/6J and CBA/Ca, The Jackson Laboratory (stock no. 001752); line 4—T9H/T9H, $Tyr^{c/c}$, mix of C57BL/6J, CBA/Ca, and CF-1 (made by mating lines 2 with 3 and then intercrossing); line

5—*Ascl2*$^{+/-}$, a mix of 129/Sv, outbred Swiss CD-1 and CF-1 [made by mating *Ascl2*$^{+/-}$ males (Guillemot *et al.* 1995) with females of line 2]. The mutation was maintained in (*Ascl2*$^{+/+}$ ♀ × *Ascl2*$^{+/-}$ ♂) matings; line 6—0/*Tg*, *Tyr*$^{c/c}$, a mix of C57BL/6J, CBA/Ca and CF-1 (made by producing founder transgenic lines as described below, then by crossing and backcrossing to line 2). The transgenes were maintained in (0/0 ♀ × 0/*Tg* ♂) matings; line 7—*Igf2*$^{-/-}$, *Tyr*$^{c/c}$, a mix of 129/SvEv and CF-1 [made by mating *Igf2*$^{+/-}$ mice (DeChiara *et al.* 1990) with line 2, then by intercrossing]; line 8—*Cdkn1c*$^{+/-}$, a mix of 129S7/SvEvBrd (129S7), C57BL/6J and CF-1 [made by mating *Cdkn1c*$^{+/-}$ males (Zhang *et al.* 1997) with females of line 2]. The mutation was maintained in (*Cdkn1c*$^{+/+}$ ♀ × *Cdkn1c*$^{+/-}$ ♂) matings; line 9—FVB/NJ.CAST/Ei(N3), which is homozygous for the *M. musculus castaneus* form of dist7 (Szabó *et al.* 2002).

Production of *Ascl2* transgenic mice: A genomic DNA clone containing the *Ascl2* gene was obtained by screening a P1 genomic DNA library—mouse strain 129XI/SvJ, vector pAD10SacBII (Genome Systems). Ends were located at 17.64 kb 5′ and 66.34 kb 3′ of the *Ascl2* ATG translation initiation codon. One end of the 84-kb insert was at 19 kb from the nearest annotated gene toward the telomere, *Tspan32* (*tetraspanin 32*). The other end was within the first intron of the nearest annotated gene toward the centromere, *Th* (*tyrosine hydroxylase*). Founder transgenic mice were made using the whole *Ascl2* P1 clone in circular form (C) or after linearization (L) with *Not*I [*e.g.*, founders *Tg(Ascl2)6C* and *-10L*, respectively]. Zygotes of strain (C57BL/6J × CBA/CaJ)F_2 were microinjected with DNA as described (Mann and McMahon 1993; Mann 1993) to obtain founder animals identified by PCR using primers specific for the pAD10SacBII vector sequence, 5′-TCTG GCAG GAGG AGCG ACTC AAG-3′ and 5′-CCGT TTTC TGTT CCCG TG-3′ (753-bp amplicon). Copy number and chromosomal location of the integration events were not investigated. Transgenic integration events (*Tg*) were tested for function by introducing them into *Ascl2* mutants. Paternal transmission was as follows: (*Ascl2*$^{+/-}$, 0/0 ♀ × *Ascl2*$^{+/+}$, 0/*Tg* ♂) matings, testing for survival to term of (*Ascl2*$^{-/+}$, 0/*Tg*) embryos. Maternal transmission was as follows: (*Ascl2*$^{+/-}$, *Tg*/0 ♀ × *Ascl2*$^{+/+}$, 0/0 ♂) matings, testing for survival to term of (*Ascl2*$^{-/+}$, *Tg*/0) embryos.

Matings: *Production of PatDp(dist7)T9H-0/Tg, Igf2*$^{+/+}$ *fetuses:* Female (T9H/+, *Tyr*$^{+/+}$, 0/0, *Igf2*$^{+/+}$) parents were bred in (line 3 ♀ × line 1 ♂ and reciprocal matings). Male (T9H/+, *Tyr*$^{c/c}$, *Tg*/0, *Igf2*$^{+/+}$) parents were bred in (line 6 ♀ × line 4 ♂) matings. Fetuses were a mix of strains C57BL/6J, CBA/Ca, and CF-1.

Production of PatDp(dist7)T9H-0/Tg, Igf2$^{+/-}$ *and recombinant -Igf2*$^{-/-}$ *and -Igf2*$^{+/+}$ *fetuses:* Female (T9H/+, *Tyr*$^{+/+}$, 0/0) parents were bred in (line 3 ♀ × line 1 ♂ and reciprocal matings). Male (T9H/+, *Tyr*$^{c/c}$, *Tg*/0, *Igf2*$^{-/+}$) parents were bred in [(line 7 ♀ × line 6 ♂) ♀ × line 4 ♂] matings. Fetuses were a mix of strains 129S1/SvImJ, C57BL/6J, CBA/Ca, 129/SvEv, and CF-1.

Genotyping: The three *Igf2* genotypes were identified by using two PCR assays, the first detecting the mutant allele, 5′-AGCC ATTC TCCT GGGA TTAG GG-3′ (intronic) and 5′-AGCA GCCG ATTG TCTG TTGT GC-3′ [within *neo* coding sequence (cds)] (~450-bp amplicon), and the second detecting the wild-type allele, 5′-TACA GTTC AAAG CCAC CACG G-3′ (intronic) and 5′-GCCA AAGA GATG AGAA GCAC CAAC-3′ (exonic) (323-bp amplicon). The *Ascl2*$^{-}$ allele was identified using primers, 5′-GCCT TCTA TCGC CTTC TTGA CG-3′ (within *neo* cds) and 5′-CCCC CTAA CCAA CTGG AAAA GTC-3′ (exonic) (~650-bp amplicon). The *Cdkn1c*$^{-}$ allele was identified using primers specific for the selection cassette used in gene targeting, 5′-CTCA GAGG CTGG GAAG GGGT GGGT C-3′ [within *Pgk1* (*phosphoglycerate kinase 1*) promoter] and 5′-ATAC TTTC TCGG CAGG AGCA AGGT G-3′ (within *neo* cds) (520-bp amplicon). The *Ascl2* transgene was identified as described above.

Gene and protein expression: Northern blots were performed as described (Szabó and Mann 1994; McLaughlin *et al.* 1996). Probes were made using the following primers: *Ascl2*, made by RT–PCR, 5′-GGCT GTTA ACAC CCGC TACT C-3′ and 5′-AGCA CTTG GCAT TTGG TCAG-3′ (356-bp amplicon); *Cdkn1c*, made by RT–PCR, 5′-GCCG GGTG ATGA GCTG GGAA-3′, and 5′-AGAG AGGC TGGT CCTT CAGC-3′ (221-bp amplicon); *Igf2* major transcript, made by RT–PCR, 5′-CCTC TCCC GTCC CTCA GTGT CA-3′ and 5′-TGTC CAGC CAAA TGGG CAGG TA-3′ (558-bp amplicon). Probes for *H19* and *Gapdh* (*glyceraldehyde-3-phosphate dehydrogenase*) transcripts were as described (Szabó and Mann 1994). Probes were hybridized independently to the same blots after stripping. Radioactivity of bands was quantified using a Typhoon biomolecular imager (GE Healthcare). For *Ascl2* quantification, values were normalized to the *Gapdh* value.

Quantitative RT–PCR single-nucleotide primer extension (SNuPE) assay for *Ascl2*, which relies on the presence of a single-nucleotide polymorphism present in an exon, was performed as described (Szabó and Mann 1995). Primers used in RT–PCR were exonic and spanned a single intron: 5′-CATA TTTT CAGT AGAG TCCT ACA-3′ and 5′-GGGA CAGA GGTC ATCT TTAT TGTG C-3′. PCR conditions were the following: (95°/45 sec, 56°/45 sec, 72°/1 min) × 33 cycles (351-bp amplicon). The SNuPE primer was 5′-CATA TTTT CAGT AGAG TCCT ACA-3′ and incorporated a radionucleotide during SNuPE, strain 129XI/SvJ—A × 1 and strain CAST/Ei—G × 1. Radioactivity of bands was quantified using a biomolecular imager as described above.

IGF2 protein concentration was measured by radioimmunoassay after removal of IGF-binding proteins by BioSpin separation, using Bio-Gel P10 (Bio-Rad) in the presence of 1 M acetic acid (Mohan and Baylink 1995). This method has been validated for measurement of IGF2 in mouse serum (Miyakoshi *et al.* 2001). Skeletons were prepared and stained with Alizarin Red S (bone) and Alcian Blue 8GX (cartilage) as described (McLeod 1980). Histological sections were stained with hematoxylin and eosin.

RESULTS

Production of a functional *Ascl2* transgene: A validated non-imprinted *Ascl2* transgene was required for restoration of *Ascl2* activity in PatDp(dist7)T9H embryos. Approximately 120 zygotes were injected with the *Ascl2* P1 clone from which six transgenic lines were derived. In all cases, the transgene (*Tg*) was transmitted in Mendelian ratios. Each independent integration event was tested for function using matings as described in MATERIALS AND METHODS. For paternal transmission, three integration events rescued mutants at the frequency expected for survival of every (*Ascl2*$^{-/+}$, 0/*Tg*) individual, or one-third of the neonates genotyped: *Tg(Ascl2)2C*, *-6C*, and *-10L*; 12/33 (36%), 11/23 (48%), and 15/44 (34%) rescued, respectively. For the remaining three lines, very low or zero frequency of survival was observed. In these cases, it is probable that the transgene was expressed at a low level relative to the endogenous gene. For maternal transmission, for each of the six lines, the frequency of survival of (*Ascl2*$^{-/+}$,

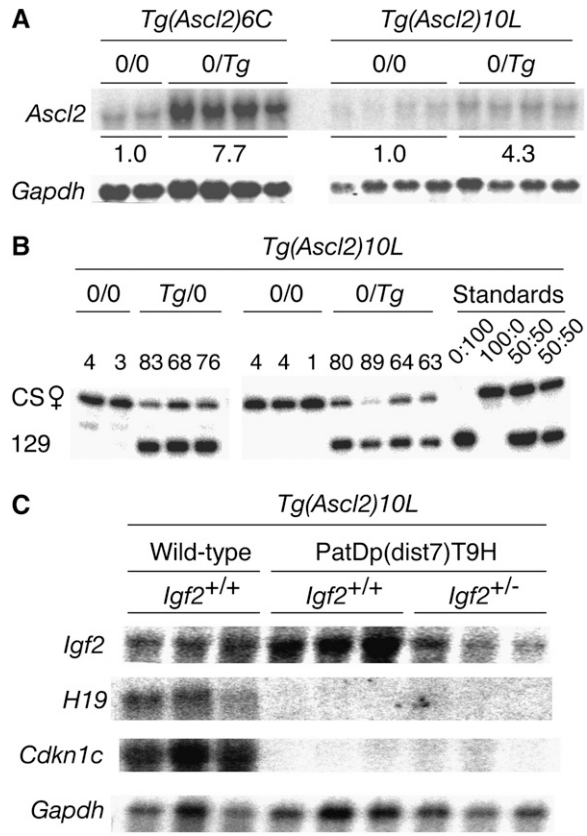

FIGURE 2.—*Ascl2* expression in placentas. (A) Northern blot. Placentas at 15½ dpc from (*Ascl2*$^{+/+}$, 0/0 ♀ × *Ascl2*$^{+/+}$, 0/*Tg* ♂) matings. Values under the bands represent the average relative amount of total *Ascl2* RNA corrected for the amount of *Gapdh* RNA determined after washing and rehybridization. (B) RT–PCR SNuPE assay to determine the ratio of allele-specific expression. Placentas at 10½ dpc from (*Ascl2*$^{+/+}$, 0/0 ♀ × *Ascl2*$^{+/+}$, 0/*Tg* ♂) and reciprocal matings. The endogenous maternal and paternal *Ascl2* alleles were derived from strain CAST/Ei (CS) and 129, respectively, while the *Tg* was also derived from strain 129. Values above each pair of bands represent the amount of 129-derived *Ascl2* RNA as the percentage of the total amount of *Ascl2* RNA present. In *Tg*/0 (*Tg* maternally derived) and 0/*Tg* (*Tg* paternally derived) embryos, the amount of *Tg*-derived RNA is on average 76% and 74% of the total, respectively. CS:129 placenta RNA. FVB/NJ.CS(N3) females homozygous for the CS form of dist7 (SZABÓ *et al.* 2002) were used in matings described above and as a source of RNA. (C) Northern blot. Placentas at 17½–18½ dpc. Three of each genotype were used, as shown.

Tg/0) embryos to term was equivalent to that obtained on paternal transmission. For the three rescuing lines, these latter results show that the transgene segregated independently of *Ascl2*. Overall, the results indicate that none of the integration events were subject to imprinting, this being expected given that imprinting of *Ascl2* is regulated by ICR2 and not by immediately adjacent sequences.

Expression of *Ascl2* was examined in two of the three rescuing lines—*Tg(Ascl2)6C* and *-10L*. In 15½ days postcoitum (dpc) transgenic placentas, Northern blots showed that the total amount of *Ascl2* RNA was 7.7 (line *-6C*) and 4.3 (line *-10L*) times greater than endogenous *Ascl2* RNA (Figure 2A). In 10½ dpc *Tg(Ascl2)10L* transgenic placentas, quantitative RT–PCR SNuPE assays showed that ~75% of the total placental *Ascl2* RNA was derived from the transgene, regardless of parental inheritance (Figure 2B). Together, these results indicate that in line *Tg(Ascl2)10L*, from 10½–15½ dpc, total *Ascl2* RNA is approximately fourfold higher than endogenous, with three-fourths of this RNA derived from the transgene. The *Tg(Ascl2)10L* transgene was selected for introduction into PatDp(dist7)T9H embryos.

Rescue of PatDp(dist7)T9H embryos by the *Ascl2* transgene and expression of imprinted genes: To produce PatDp(dist7)T9H zygotes, (T9H/+, *Tyr*$^{+/+}$, 0/0 ♀ × T9H/+, *Tyr*$^{c/c}$, *Tg*/0 ♂) matings were performed (Figure 3A). One in two PatDp(dist7)T9H zygotes would inherit *Tg* and not be subject to ASCL2 deficiency. If viable, they would be identifiable from 12½ days dpc as albinos, lacking in eye and fur pigmentation, as they must be homozygous for the dist7 marker, albino (*c*), a mutation of the *Tyr* (tyrosinase) gene. At 13½–18½ dpc, albino or PatDp(dist7)T9H fetuses were observed at approximately the frequency expected—one in 15—and all carried the *Ascl2* transgene. These PatDp(dist7)T9H-0/*Tg*, *Tyr*$^{c/c}$ fetuses would be expected to have two active alleles of *Igf2* and to overexpress this gene. To normalize the level of *Igf2* transcript, (T9H/+, *Tyr*$^{+/+}$, 0/0, *Igf2*$^{+/+}$ ♀ × T9H/+, *Tyr*$^{c/c}$, *Tg*/0, *Igf2*$^{-/+}$ ♂) matings were also performed, which would produce PatDp(dist7)T9H-0/*Tg*, *Tyr*$^{c/c}$, *Igf2*$^{+/-}$ and also recombinant *-Igf2*$^{+/+}$ and *-Igf2*$^{-/-}$ zygotes (Figure 3B).

In late-term PatDp(dist7)T9H-0/*Tg* fetuses that were recovered, the expression levels of *Igf2*, *H19*, and *Cdkn1c* in the placenta were assessed in Northern blots. As expected, PatDp(dist7)T9H-0/*Tg*, *Igf2*$^{+/+}$, and *-Igf2*$^{+/-}$ placentas lacked *H19* and *Cdkn1c* expression, with the former apparently having excess *Igf2* expression, and the latter, a normal amount of transcript (Figure 2C). Fetal serum IGF2 protein concentrations reflected the level of transcript and are expressed in nanograms per microliter: controls—four wild-type *Igf2*$^{+/+}$ fetuses (153, 153, 147, and 174), three mutant *Igf2*$^{+/-}$ fetuses lacking *Igf2* RNA (60, 63, 66), equivalent to background concentration; experimentals—two PatDp(dist7)T9H, 0/*Tg*, *Igf2*$^{+/+}$ fetuses (180, 186), two PatDp(dist7)T9H-0/*Tg*, *Igf2*$^{+/-}$ fetuses (120, 138), and one PatDp(dist7)T9H-0/*Tg*, *Igf2*$^{-/-}$ fetus (48). Therefore PatDp(dist7)T9H, 0/*Tg*, *Igf2*$^{+/+}$ and *-Igf2*$^{+/-}$ fetuses had ~1.3- and 0.7-fold the normal concentration of serum IGF2, respectively. Despite the high frequency of rescue of PatDp(dist7)T9H fetuses at late term by the *Ascl2* transgene, the phenotype of these fetuses was not completely normalized as the effects of other misexpressions had come into play.

Defects in perinatal PatDp(dist7)T9H, 0/*Tg* fetuses and newborns: The expected frequency of recovery of

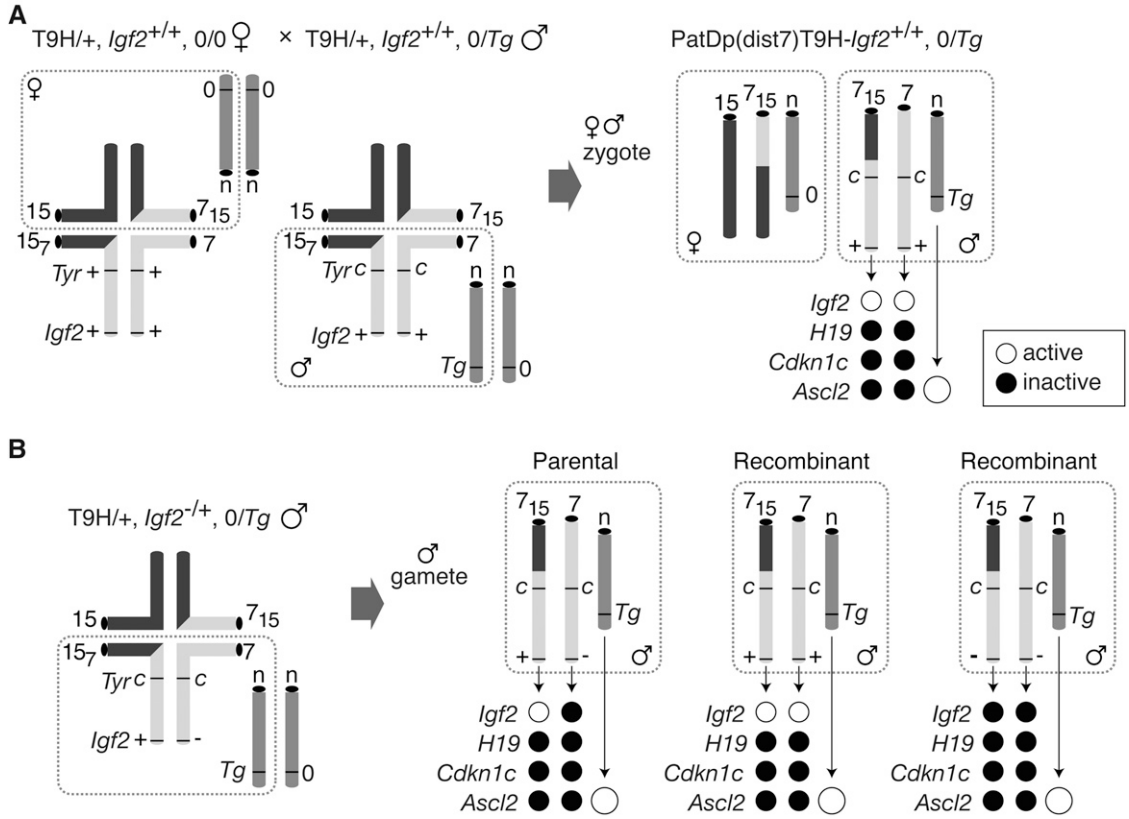

FIGURE 3.—Production of PatDp(dist7)T9H fetuses and allele-specific expression. (A) Quadrivalents at meiosis in translocation heterozygotes (T9H/+). Male parent is *Igf2*$^{+/+}$, *Tyr*$^{c/c}$, or albino and *Tg*/0 with *Tg* on an unknown autosome (n). The female parent is *Tyr*$^{+/+}$ and does not carry *Tg* (0/0). Unbalanced complementary gametes (dashed boundaries) combine to give PatDp(dist7)T9H-0/*Tg* zygotes identified as albinos. Half of the PatDp(dist7)T9H zygotes will be 0/0 with respect to *Tg* and therefore cannot develop beyond 10½ dpc. Expected activity state of an allele is indicated by a solid circle (inactive) or an open circle (active). Expression of *Ascl2* derived from *Tg* is greater than for the endogenous allele (larger circles). (B) Quadrivalent at meiosis in male T9H/+, *Igf2*$^{+/-}$ parents, which were mated to the same females as in A. The three types of gametes produced are depicted: *Igf2*$^{+/-}$ (parental) and *Igf2*$^{+/+}$ or *Igf2*$^{-/-}$ (recombinants). Chromosomes depicted are actually paired chromatids. Other details as in A.

PatDp(dist7)T9H-0/*Tg* zygotes is ~1 in 50 and is further complicated by small litter sizes due to the death of the majority of ova at peri-implantation due to chromosome imbalance. It is therefore difficult to obtain sufficient numbers and material for in-depth analysis of phenotype. Nevertheless, consistent abnormalities were observed. While wild-type placenta carrying *Tg* were normal in appearance (Figure 4A), PatDp(dist7)T9H-0/*Tg*, *Igf2*$^{+/+}$ displayed a pronounced placentamegaly, often being at least twofold heavier with increased proportions compared to wild-type uterus mates (Figure 5, E and F, Figure 6). Placentamegaly was also seen in PatDp(dist7)T9H-0/Tg, *Igf2*$^{+/-}$ and -*Igf2*$^{-/-}$ fetuses, although possibly was not as marked (Figure 6). Additional -*Igf2*$^{+/-}$ and *Igf2*$^{-/-}$ individuals were obtained that confirmed the presence of this defect (data not shown), and histological examination revealed a disorganization of labyrinth and spongiotrophoblast possibly due to the presence of greatly enlarged maternal blood sinuses filled with red blood cells (Figure 4, B and C).

All PatDp(dist7)T9H-0/*Tg*, *Igf2*$^{+/+}$ and -*Igf2*$^{+/-}$ rescued fetuses were stout or thickset in appearance (Figure 5, B and C). Stoutness is consistent with CDKN1C deficiency, but the absence of this feature in all of the three PatDp(dist7)T9H-0/*Tg*, *Igf2*$^{-/-}$ fetuses recovered (Figure 5D) indicates that this defect is also dependent on the presence of IGF2. In PatDp(dist7)T9H-0/*Tg*, *Igf2*$^{+/+}$ fetuses, abnormalities consistent with IGF2 excess included increased weight relative to wild-type uterus mates, although the small numbers obtained do not allow for statistical analysis of significance (Figure 6). They were not longer, as crown-rump length was not relatively increased (Figure 6). In PatDp(dist7)T9H-0/*Tg*, *Igf2*$^{+/-}$ fetuses, in which IGF2 concentrations were normalized, insufficient numbers were obtained to determine if they were of normal weight. Polydactyly was seen in every PatDp(dist7)T9H-0/Tg, *Igf2*$^{+/+}$ and -*Igf2*$^{+/-}$ fetus recovered. Eyelid fusion failure or open eyes occurred in four of five PatDp(dist7)T9H-0/Tg, *Igf2*$^{+/+}$ and in two of seven PatDp

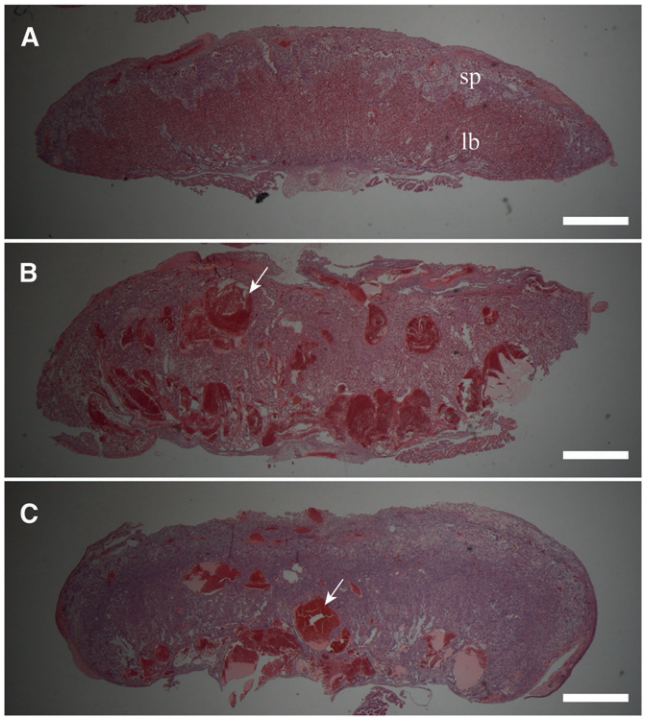

FIGURE 4.—Placenta phenotype in PatDp(dist7)T9H-0/*Tg* fetuses. (A) Wild-type 0/*Tg*, *Igf2*$^{+/+}$. sp, 17½ dpc spongiotrophoblast layer; lb, labyrinth trophoblast layer. (B) PatDp(dist7)T9H-0/*Tg*, *Igf2*$^{+/-}$ 17½ dpc. A portion of this placenta was removed for RNA extraction. (C) PatDp(dist7)T9H-0/*Tg*, *Igf2*$^{-/-}$, 18½ dpc. Bars, 1 mm.

(dist7)T9H-0/*Tg*, *Igf2*$^{+/-}$ rescued fetuses. None of three PatDp(dist7)T9H-0/*Tg*, *Igf2*$^{-/-}$ fetuses possessed polydactyly or open eyes, indicating that these defects were dependent on IGF2. Some of these fetuses are further described (Figure 5, B–D, Figure 6).

Most PatDp(dist7)T9H-0/*Tg*, *Igf2*$^{+/+}$ and -*Igf2*$^{+/-}$ fetuses possessed abdominal abnormalities in the form of thinned abdominal skin or muscle wall through which the liver and gut could be easily discerned. Often this was accompanied by a hernia adjacent to the umbilicus, with or without protrusion of intestines or omphalocele (Figure 5L). The distension of the abdomen in PatDp(dist7)T9H-0/*Tg*, *Igf2*$^{+/+}$ fetuses appeared to be caused by an enlarged liver (Figure 5, L and N). In all viable PatDp(dist7)T9H-0/*Tg*, *Igf2*$^{+/+}$ and -*Igf2*$^{+/-}$ fetuses and controls, the gut was removed and straightened. Unexpectedly, in all cases, it was of normal morphology and was not shortened as usually seen in *Cdkn1c* mutants (YAN *et al.* 1997; ZHANG *et al.* 1997).

PatDp(dist7)T9H-0/*Tg* fetuses of all three *Igf2* genotypes possessed shortened limbs (Figure 5, B and D); this defect was consistent with the reduced chondrogenesis associated with CDKN1C deficiency (YAN *et al.* 1997; ZHANG *et al.* 1997). Unexpectedly, no PatDp(dist7)T9H-0/*Tg* fetus possessed cleft palate (Figure 5I), a common defect in *Cdkn1c* mutants (Figure 5J) (YAN *et al.* 1997; ZHANG *et al.* 1997). Differential staining of bone and cartilage revealed a generalized hypo-ossification of the skull, vertebrae, limbs, and ribs accompanied by bifurcation of the sternum (Figure 7, E–H). Thus, reduced chondrogenesis and hypo-ossification are as penetrant in PatDp(dist7)T9H-0/*Tg* fetuses as in *Cdkn1c* mutants (Figure 7, I–L), although not as severe. The same severity of defects was seen in all of four additional PatDp(dist7)T9H-0/*Tg* fetuses and newborns—one -*Igf2*$^{+/+}$ and three -*Igf2*$^{+/-}$ (data not shown).

DISCUSSION

When provided with a functional *Ascl2* transgene, PatDp(dist7)T9H embryos were able to develop to the latest stages of gestation, providing strong evidence that the death of PatDp(dist7)T9H embryos at midgestation is the result of two epigenetically inactivated endogenous copies of the *Ascl2* gene. A contribution from other misexpressions in their death cannot be entirely ruled out, as the *Ascl2* transgene used was overexpressed and in other ways may not have been expressed exactly in accord with the endogenous gene. Such nonphysiological *Ascl2* expression could compensate in some way for other existent misexpressions. The degree of survival after restoration of *Ascl2* expression is remarkable, given the potent effects of PatDp(dist7)T9H ES cells in chimeras (MCLAUGHLIN *et al.* 1997). The present experiments extend these previous observations of chimeras by allowing for the assessment of the effects of PatDp(dist7)T9H when non-mosaic, of the contribution of excess IGF2 to the phenotype, and of the effect of PatDp(dist7)T9H on placental development, which is not possible with ES cells as they do not colonize the trophoblast.

The phenotype of PatDp(dist7)T9H-0/*Tg*, *Igf2*$^{+/+}$ fetuses results from the combined action of all misexpressed imprinted genes located at dist7 and is likely to have a complex etiology. For placentamegaly, a partial explanation is lack of *Cdkn1c* expression, as *Cdkn1c* mutant placentas are 1.4-fold heavier than wild type (TAKAHASHI *et al.* 2000). In PatDp(dist7)T9H-0/*Tg*, *Igf2*$^{+/+}$ fetuses, the greater increase in size, together with labyrinth or spongiotrophoblast disorganization and enlarged maternal blood sinuses, can be sufficiently explained by CDKN1C deficiency together with IGF2 excess: When this specific combination of misexpressions is brought about through genetic modification, a similar phenotype results (CASPARY *et al.* 1999). Nevertheless, in PatDp(dist7)T9H fetuses, other misexpressions must be involved as placentamegaly persisted in PatDp(dist7)T9H-0/*Tg*, *Igf2*$^{+/-}$ and -*Igf2*$^{-/-}$ fetuses. A good candidate for this effect is the inactivity of the maternally expressed *Phlda2* (pleckstrin homology-like domain, family A, member 2) gene, regulated by ICR2. This gene is a negative regulator of placental growth, with *Phlda2* null mice having greatly enlarged placentas

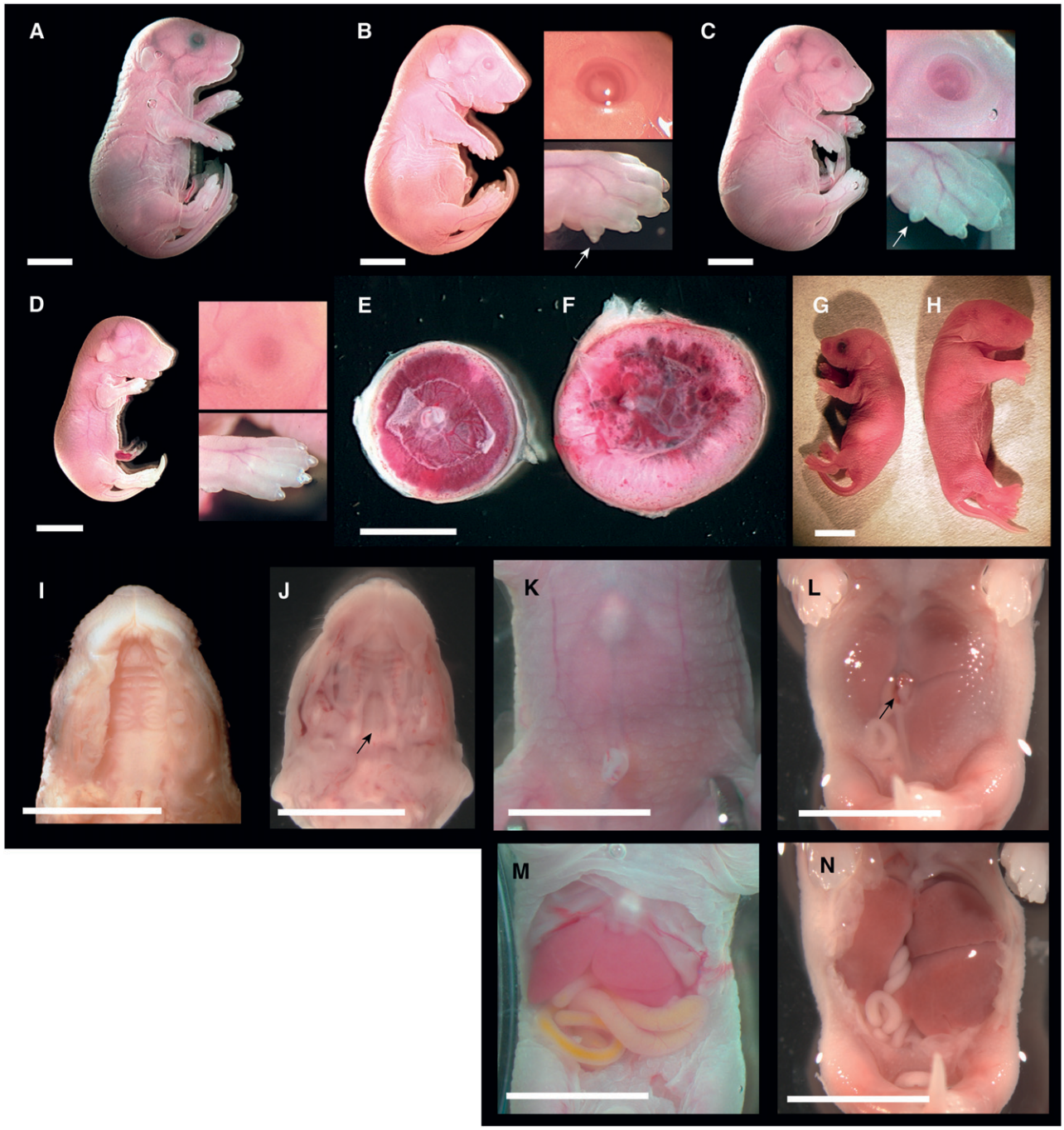

FIGURE 5.—Overt phenotype of late-term PatDp(dist7)T9H-0/*Tg* fetuses. (A) Fetus, 18½ dpc, wild type. (B) Fetus, 18½ dpc, PatDp(dist7)T9H-0/*Tg*, $Igf2^{+.+}$; insets show eye and forepaw, with arrow indicating additional digit or polydactyly. (C) Fetus, 18½ dpc, PatDp(dist7)T9H-0/*Tg*, $Igf2^{+/-}$, insets and arrow as for B. (D) Fetus, 18½ dpc, PatDp(dist7)T9H-0/*Tg*, $Igf2^{-/-}$, insets as for B. (E) Placenta, 16½ dpc, wild type. (F) Placenta, 16½ dpc, PatDp(dist7)T9H-0/*Tg*, $Igf2^{+/+}$, uterus mate to E. (G) Neonate, ½ days post partum (dpp), $Igf2^{+/-}$. (H) Neonate, ½ dpp, PatDp(dist7)T9H-0/*Tg*, $Igf2^{+/-}$. (I) Exposed palate, 18½ dpc, PatDp(dist7)T9H-0/*Tg*, $Igf2^{+/+}$. (J) Exposed palate, 17½ dpc, $Cdkn1c^{-/+}$. Arrow indicates cleft in palate. (K) Abdomen, 18½ dpc, wild type. (L) Abdomen, 18½ dpc, PatDp(dist7)T9H-0/*Tg*, $Igf2^{+/+}$. Arrow indicates hernia adjacent to the umbilicus. (M) Exposed abdomen of K. (N) Exposed abdomen of L. Bars, 0.5 cm.

(FRANK *et al.* 2002). There are a number of other candidates, as most if not all imprinted genes under regulatory control of ICR2 are expressed in the placenta (COAN *et al.* 2005) and are likely to be inactive in PatDp(dist7)T9H-0/*Tg* conceptuses. Also, other dist7 imprinted genes are expressed in the placenta and are not regulated by ICR1 or ICR2 (SCHULZ *et al.* 2006). Finally, it is conceivable that the threefold extra *Ascl2* RNA derived from the *Ascl2* transgene may have contributed to the placental phenotype. However,

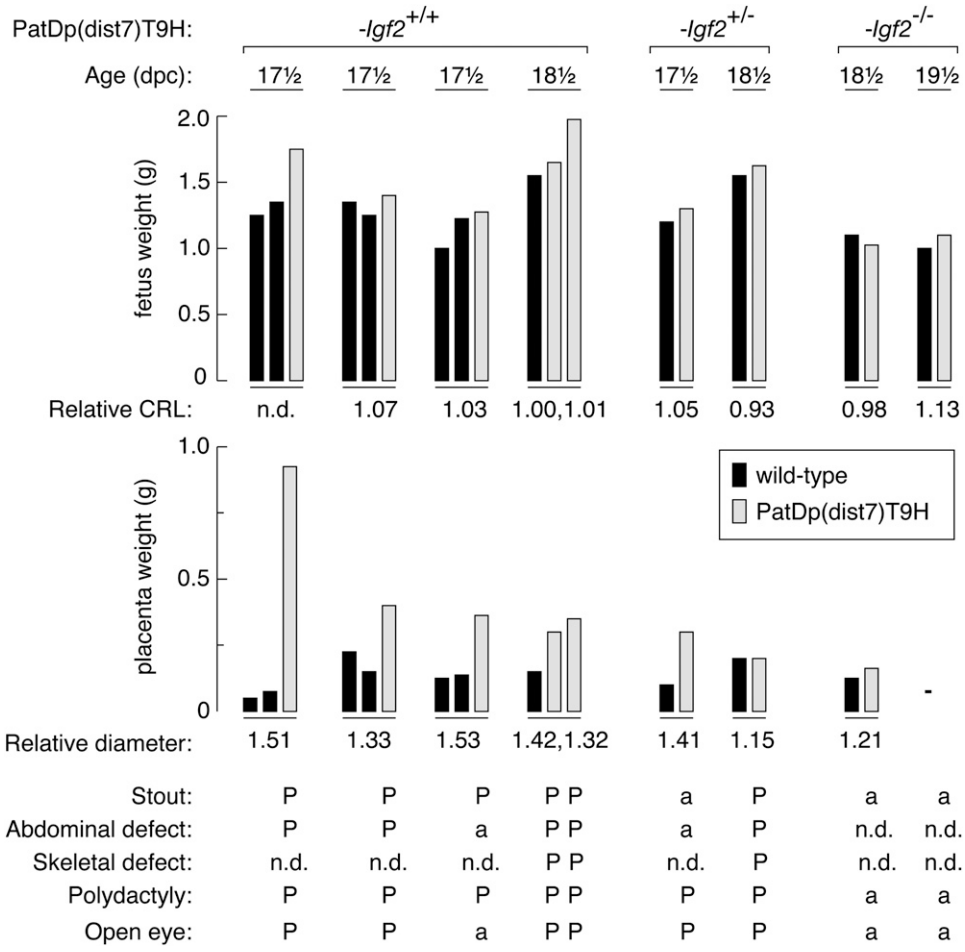

FIGURE 6.—Summary of phenotypic defects in PatDp(dist7)T9H-0/*Tg* fetuses. PatDp(dist7)T9H fetuses (shaded bars), with *Igf2* genotype as indicated at top, are grouped with wild-type uterus mates (solid bars). Phenotypic features for each individual are indicated from top to bottom. Relative CRL (crown-rump length) and relative diameter (for placenta) is the value obtained for PatDp(dist7)T9H divided by the value obtained for wild type. P, defect present; a, defect absent. n.d., not done; —, not applicable (the 19½ dpc PatDp(dist7)T9H-0/*Tg*, $Igf2^{-/-}$ individual and its wild-type littermate were newborns, and therefore the placenta was not measured).

wild-type fetuses carrying *Tg* had overtly normal placentas, as did *Tg(Ascl2)6C* fetuses in which expression of the transgene was at least sixfold greater than endogenous *Ascl2* RNA.

That *Tg(Ascl2)6C* and *-10L* placentas were able to develop apparently normally in the presence of an appreciable excess of *Ascl2* RNA suggests that precise regulation of ASCL2 is not crucial for trophoblast proliferation and differentiation. This finding is of interest given that previous studies have indicated that suppression of ASCL2 function is required for trophoblast giant cell (TGC) differentiation. While this suppression is thought to be brought about by the action of MDFI (MyoD family inhibitor) (KRAUT *et al.* 1998), experiments in cultured rat trophoblast cells indicate that excess ASCL2 can override the suppressive mechanism (SCOTT *et al.* 2000). *Tg(Ascl2)* mice could provide a useful tool to further investigate the importance of ASCL2 levels in TGC differentiation.

While occasional PatDp(dist7)T9H-0/*Tg* newborns were obtained, survival beyond this stage is very unlikely, given their phenotype. A number of defects seen in the PatDp(dist7)T9H-0/*Tg* fetus proper were consistent with CDKN1C deficiency, with abdominal defects, hypo-ossification, and short limbs prominent in PatDp(dist7)T9H-0/*Tg*, $Igf2^{+/+}$, and $-Igf2^{+/-}$ fetuses. However, CDKN1C deficiency-associated defects of cleft palate and gut shortening were absent, regardless of *Igf2* genotype. The reasons for these conspicuous deviations from the standard *Cdkn1c* null phenotype are unclear, but it is conceivable that a small number of cells located in important proliferation zones at least partially dispense with imprinting-regulated expression. If so, then *Cdkn1c* expression would be higher when two paternal wild-type alleles are present, PatDp(dist7)T9H, in comparison to one, $Cdkn1c^{-/+}$. This is conceivable given that the imprinting is not always tightly regulated at the tissue-specific level, for example (LEE *et al.* 1997). That genetic background may have influenced the result is unlikely, given that cleft palate and gut abnormalities are penetrant in *Cdkn1c* mutants in a variety of mixed strain backgrounds (YAN *et al.* 1997; ZHANG *et al.* 1997).

The defects of polydactyly and open eyes in PatDp(dist7)T9H-0/*Tg*, $Igf2^{+/+}$, and $-Igf2^{+/-}$ fetuses are associated with excess IGF2. Polydactyly has been described in mice with biallelic expression of *Igf2* (EGGENSCHWILER *et al.* 1997; SZABÓ *et al.* 2004), and both defects are seen in fetuses with IGF2 super-excess; this occurs when biallelic expression of *Igf2* is combined in the same fetus with lack of activity of the chromosome 17 *Igf2r* (*insulin like growth factor 2 receptor*) gene (EGGENSCHWILER *et al.* 1997). Given the apparent dependency of these defects on excess

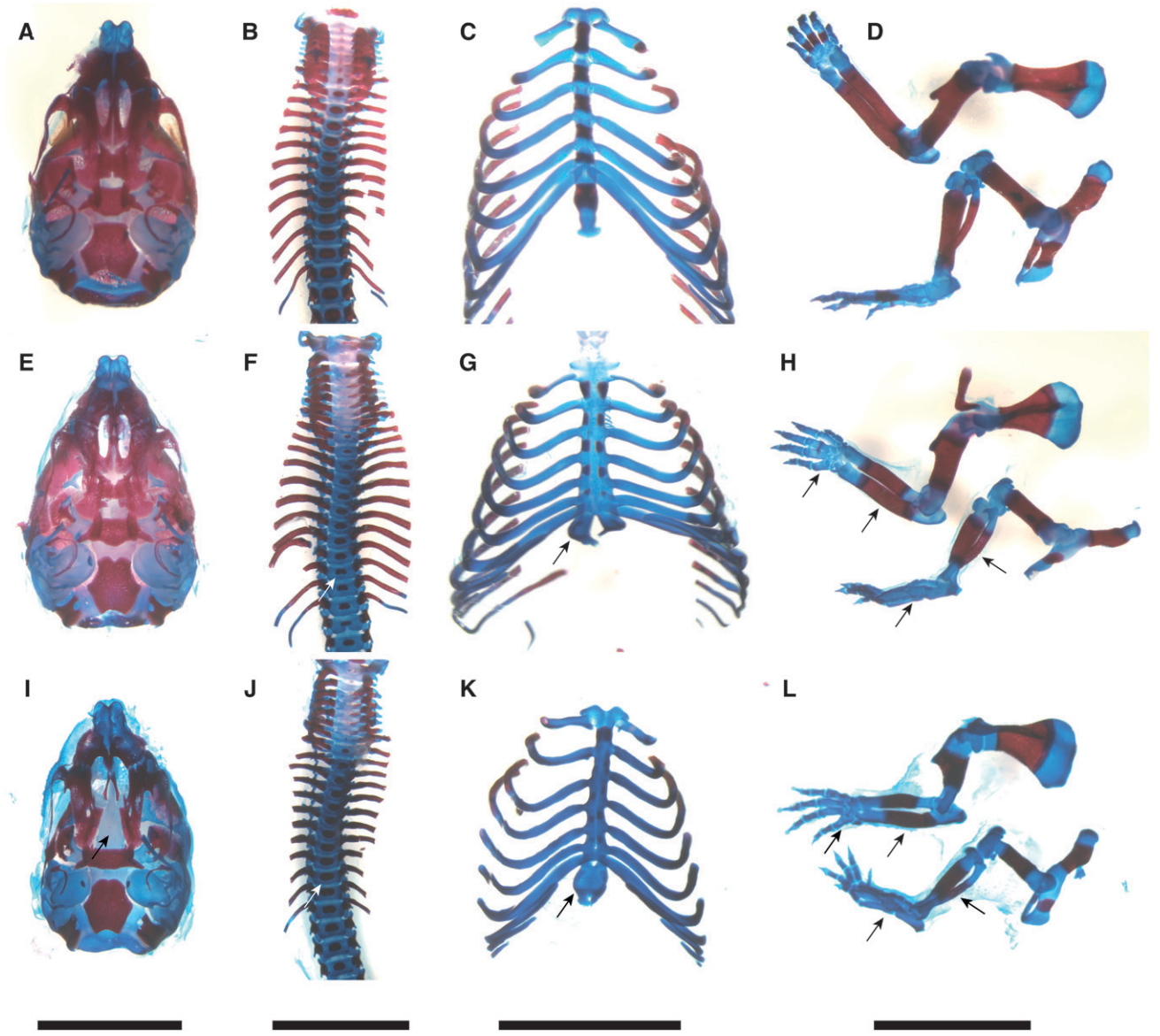

FIGURE 7.—Phenotype of skeleton in late-term PatDp(dist7)T9H-0/*Tg* fetuses. (A–D) Wild type. (E–H) PatDp(dist7)T9H-*Igf2*$^{+/-}$, 0/*Tg*. (I–L) *Cdkn1c*$^{-/+}$. (A, E, and I) Skull, ventral surface. (B, F, and J) Spine. (C, G, and K) Ribcage. (D, H, and L) Forelimb (top); hindlimb (bottom). Bone, stained red; cartilage, stained blue. Prominent features, as indicated by arrows, include cleft palate (I), smaller ossification centers in vertebrae (F and J), bifurcated sternum (G and K), shorter bone length in forelimbs and hindlimbs and hypo-ossification in phalanges (H and L). Bars, 0.5 cm.

IGF2, their occurrence was unexpected in PatDp (dist7)T9H-0/*Tg*, *Igf2*$^{+/-}$ fetuses in which IGF2 concentrations were normalized. Similar to placentamegaly, these results point to a role for misexpressions other than CDKN1C deficiency and IGF2 excess in the etiology, although these defects appear to have a partial requirement for IGF2 as they were not observed in PatDp (dist7)T9H-0/*Tg*, *Igf2*$^{-/-}$ fetuses. Hepato- and cardiomegaly were reported in PatDp(dist7)T9H ES cell chimeras (McLAUGHLIN *et al.* 1997), and at least the former appeared to be present in PatDp(dist7)T9H-0/*Tg*, *Igf2*$^{+/+}$ fetuses. Again, lack of expression of the negative growth regulator *Phlda2* may play a role. Normally, *Phlda2* is expressed and imprinted in liver, lung, and kidney, and while its lack of expression does not lead to a discernible phenotype in the fetus (FRANK *et al.* 2002), it might cause pathology when combined with other misexpressions.

This genetic analysis provides implications for Beckwith–Wiedemann syndrome, a disease commonly associated with sporadic epigenetic lesions at the dist7 orthologous chromosome region, 11p15.5. Defects observed are placentamegaly, macrosomia, organomegaly including macroglossia, abdominal defects, and a high incidence of childhood cancer. We note that *ASCL2*, while located at 11p15.5, is not imprinted in humans (WESTERMAN *et al.* 2001) and therefore probably has no relevance for this disease. On the basis of mouse models

(Eggenschwiler *et al.* 1997; Sun *et al.* 1997; Caspary *et al.* 1999) and familial cases of the disease, it is thought that much of the syndrome can be explained by CDKN1C deficiency, IGF2 excess, or both (Lam *et al.* 1999; DeBaun *et al.* 2002; Cooper *et al.* 2005; Enklaar *et al.* 2006). As discussed above, much of the pathology in PatDp (dist7)T9H-0/*Tg* fetuses is consistent with the same etiology. However, the observed deviations from this theme are strongly indicative of roles for unknown misexpressions in the PatDp(dist7)T9H phenotype and imply that the same may be true for the human disease.

These findings show that *Ascl2* is probably the only imprinted gene in the genome for which PatDp causes early embryonic death. This finding emphasizes and clarifies the concept that the peri-implantation death of androgenones is the synergistic result of a number of misexpressions, which remain undefined. There is evidence that disruption of the expression of one imprinted gene can affect the expression of others (Varrault *et al.* 2006; Gabory *et al.* 2009). A parallel situation is likely to be true for parthenogenones. For MatDp, the earliest stage of death is brought about by MatDp of proximal chromosome 6 and is likely mediated by inactivity of the *Peg10* (*paternally expressed 10*) gene. Like *Ascl2* mutants and PatDp(dist7)T9H embryos, *Peg10* mutants lack placental spongiotrophoblast (Ono *et al.* 2006; Williamson *et al.* 2010). It is intriguing that, for MatDp and PatDp, the earliest acting single imprinted gene misexpression that results in a developmental barrier involves the silencing of a gene essential for the viability of the same tissue at the same developmental stage. In both cases, the extra-embryonic tissues could be primarily affected because parthenogenetic and androgenetic epiblasts appear intrinsically viable, given that ES cell lines can be readily derived from either (Robertson 1987; Mann *et al.* 1990). It would seem advantageous, or at least convenient, for mice for imprinting to act to prevent the development of uniparental embryos beyond the peri-implantation stage, thereby conserving valuable reproductive resources.

We thank Andras Nagy for the *Ascl2* knockout mouse line, Elizabeth Robertson and Agiris Efstratiadis for the *Igf2* knockout mouse line, James Cross and Stephen Elledge for the *Cdkn1c* knockout mouse line, and Trevelyan Menheniott for stimulating discussions. This work was supported by the National Institutes of Health and the National Health and Medical Research Council of Australia.

LITERATURE CITED

Avise, J. C., 2008 *Clonality: The Genetics, Ecology, and Evolution of Sexual Abstinence in Vertebrate Animals*. Oxford University Press, New York.

Barton, S. C., M. A. Surani and M. L. Norris, 1984 Role of paternal and maternal genomes in mouse development. Nature **311:** 374–376.

Beechey, C. V., S. T. Ball, K. M. Townsend and J. Jones, 1997 The mouse chromosome 7 distal imprinting region maps to G-bands F4/F5. Mamm. Genome **8:** 236–240.

Bell, A. C., and G. Felsenfeld, 2000 Methylation of a CTCF-dependent boundary controls imprinted expression of the Igf2 gene. Nature **405:** 482–485.

Caspary, T., M. A. Cleary, E. J. Perlman, P. Zhang, S. J. Elledge *et al.*, 1999 Oppositely imprinted genes p57(Kip2) and igf2 interact in a mouse model for Beckwith-Wiedemann syndrome. Genes Dev. **13:** 3115–3124.

Cattanach, B. M., and C. V. Beechey, 1997 Genomic imprinting in the mouse: possible final analysis, pp. 118–145 in *Genomic Imprinting*, edited by W. Reik and A. Surani. IRL Press, Oxford.

Cattanach, B. M., and M. Kirk, 1985 Differential activity of maternally and paternally derived chromosome regions in mice. Nature **315:** 496–498.

Coan, P. M., G. J. Burton and A. C. Ferguson-Smith, 2005 Imprinted genes in the placenta: a review. Placenta **26**(Suppl. A): S10–S20.

Cooper, W. N., A. Luharia, G. A. Evans, H. Raza, A. C. Haire *et al.*, 2005 Molecular subtypes and phenotypic expression of Beckwith-Wiedemann syndrome. Eur. J. Hum. Genet. **13:** 1025–1032.

DeBaun, M. R., E. L. Niemitz, D. E. McNeil, S. A. Brandenburg, M. P. Lee *et al.*, 2002 Epigenetic alterations of H19 and LIT1 distinguish patients with Beckwith-Wiedemann syndrome with cancer and birth defects. Am. J. Hum. Genet. **70:** 604–611.

DeChiara, T. M., A. Efstratiadis and E. J. Robertson, 1990 A growth-deficiency phenotype in heterozygous mice carrying an insulin-like growth factor II gene disrupted by targeting. Nature **345:** 78–80.

Eggenschwiler, J., T. Ludwig, P. Fisher, P. A. Leighton, S. M. Tilghman *et al.*, 1997 Mouse mutant embryos overexpressing IGF-II exhibit phenotypic features of the Beckwith-Wiedemann and Simpson-Golabi-Behmel syndromes. Genes Dev. **11:** 3128–3142.

Enklaar, T., B. U. Zabel and D. Prawitt, 2006 Beckwith-Wiedemann syndrome: multiple molecular mechanisms. Expert Rev. Mol. Med. **8:** 1–19.

Fitzpatrick, G. V., P. D. Soloway and M. J. Higgins, 2002 Regional loss of imprinting and growth deficiency in mice with a targeted deletion of KvDMR1. Nat. Genet. **32:** 426–431.

Fowden, A. L., C. Sibley, W. Reik and M. Constancia, 2006 Imprinted genes, placental development and fetal growth. Horm. Res. **65**(Suppl. 3): 50–58.

Frank, D., W. Fortino, L. Clark, R. Musalo, W. Wang *et al.*, 2002 Placental overgrowth in mice lacking the imprinted gene Ipl. Proc. Natl Acad. Sci. USA **99:** 7490–7495.

Gabory, A., M. A. Ripoche, A. Le Digarcher, F. Watrin, A. Ziyyat *et al.*, 2009 H19 acts as a trans regulator of the imprinted gene network controlling growth in mice. Development **136:** 3413–3421.

Guillemot, F., T. Caspary, S. M. Tilghman, N. G. Copeland, D. J. Gilbert *et al.*, 1995 Genomic imprinting of Mash2, a mouse gene required for trophoblast development. Nat. Genet. **9:** 235–242.

Han, L., P. E. Szabó and J. R. Mann, 2010 Postnatal survival of mice with maternal duplication of distal chromosome 7 induced by a Igf2/H19 imprinting control region lacking insulator function. PLoS Genet. **6:** e1000803.

Hark, A. T., C. J. Schoenherr, D. J. Katz, R. S. Ingram, J. M. Levorse *et al.*, 2000 CTCF mediates methylation-sensitive enhancer-blocking activity at the H19/Igf2 locus. Nature **405:** 486–489.

Hudson, Q. J., T. M. Kulinski, S. P. Huetter and D. P. Barlow, 2010 Genomic imprinting mechanisms in embryonic and extraembryonic mouse tissues. Heredity **105:** 45–56.

Kraut, N., L. Snider, C.-M. A. Chen, S. J. Tapscott and M. Groudine, 1998 Requirement of the mouse I-mfa gene for placental development and skeletal patterning. EMBO J. **17:** 6276–6288.

Lam, W. W., I. Hatada, S. Ohishi, T. Mukai, J. A. Joyce *et al.*, 1999 Analysis of germline CDKN1C (p57KIP2) mutations in familial and sporadic Beckwith-Wiedemann syndrome (BWS) provides a novel genotype-phenotype correlation. J. Med. Genet. **36:** 518–523.

Lee, M. P., R. J. Hu, L. A. Johnson and A. P. Feinberg, 1997 Human KVLQT1 gene shows tissue-specific imprinting and encompasses Beckwith-Wiedemann syndrome chromosomal rearrangements. Nat. Genet. **15:** 181–185.

Mancini-Dinardo, D., S. J. Steele, J. M. Levorse, R. S. Ingram and S. M. Tilghman, 2006 Elongation of the Kcnq1ot1 transcript is required for genomic imprinting of neighboring genes. Genes Dev. **20:** 1268–1282.

Mann, J. R., 1993 Surgical techniques in production of transgenic mice. Methods Enzymol. **225:** 782–793.

Mann, J. R., and R. H. Lovell-Badge, 1984 Inviability of parthenogenones is determined by pronuclei, not egg cytoplasm. Nature **310:** 66–67.

Mann, J. R., and A. P. McMahon, 1993 Factors influencing production frequency of transgenic mice. Methods Enzymol. **225:** 771–781.

Mann, J. R., I. Gadi, M. L. Harbison, S. J. Abbondanzo and C. L. Stewart, 1990 Androgenetic mouse embryonic stem cells are pluripotent and cause skeletal defects in chimeras: implications for genetic imprinting. Cell **62:** 251–260.

McGrath, J., and D. Solter, 1984 Completion of mouse embryogenesis requires both the maternal and paternal genomes. Cell **37:** 179–183.

McLaughlin, K. J., P. Szabó, H. Haegel and J. R. Mann, 1996 Mouse embryos with paternal duplication of an imprinted chromosome 7 region die at midgestation and lack placental spongiotrophoblast. Development **122:** 265–270.

McLaughlin, K. J., H. Kochanowski, D. Solter, G. Schwarzkopf, P. E. Szabó *et al.*, 1997 Roles of the imprinted gene Igf2 and paternal duplication of distal chromosome 7 in the perinatal abnormalities of androgenetic mouse chimeras. Development **124:** 4897–4904.

McLeod, M. J., 1980 Differential staining of cartilage and bone in whole mouse fetuses by alcian blue and alizarin red S. Teratology **22:** 299–301.

Miyakoshi, N., C. Richman, Y. Kasukawa, T. A. Linkhart, D. J. Baylink *et al.*, 2001 Evidence that IGF-binding protein-5 functions as a growth factor. J. Clin. Invest. **107:** 73–81.

Mohan, S., and D. J. Baylink, 1995 Development of a simple valid method for the complete removal of insulin-like growth factor (IGF)-binding proteins from IGFs in human serum and other biological fluids: comparison with acid-ethanol treatment and C18 Sep-Pak separation. J. Clin. Endocrinol. Metab. **80:** 637–647.

Ono, R., K. Nakamura, K. Inoue, M. Naruse, T. Usami *et al.*, 2006 Deletion of Peg10, an imprinted gene acquired from a retrotransposon, causes early embryonic lethality. Nat. Genet. **38:** 101–106.

Renfree, M. B., T. A. Hore, G. Shaw, J. A. Graves and A. J. Pask, 2009 Evolution of genomic imprinting: insights from marsupials and monotremes. Annu. Rev. Genomics Hum. Genet. **10:** 241–262.

Robertson, E. J., 1987 Embryo-derived stem cell lines, pp. 71–112 in *Teratocarcinomas and Embryonic Stem Cells. A Practical Approach*, edited by E. J. Robertson. IRL Press, Oxford/Washington, DC.

Schulz, R., T. R. Menheniott, K. Woodfine, A. J. Wood, J. D. Choi *et al.*, 2006 Chromosome-wide identification of novel imprinted genes using microarrays and uniparental disomies. Nucleic Acids Res. **34:** e88.

Scott, I. C., L. Anson-Cartwright, P. Riley, D. Reda and J. C. Cross, 2000 The HAND1 basic helix-loop-helix transcription factor regulates trophoblast differentiation via multiple mechanisms. Mol. Cell. Biol. **20:** 530–541.

Searle, A. G., and C. V. Beechey, 1990 Genomic imprinting phenomena on mouse chromosome 7. Genet. Res. **56:** 237–244.

Shin, J. Y., G. V. Fitzpatrick and M. J. Higgins, 2008 Two distinct mechanisms of silencing by the KvDMR1 imprinting control region. EMBO J. **27:** 168–178.

Solter, D., 2006 Imprinting today: End of the beginning or beginning of the end? Cytogenet. Genome Res. **113:** 12–16.

Sun, F. L., W. L. Dean, G. Kelsey, N. D. Allen and W. Reik, 1997 Transactivation of Igf2 in a mouse model of Beckwith-Wiedemann syndrome. Nature **389:** 809–815.

Surani, M. A., S. C. Barton and M. L. Norris, 1984 Development of reconstituted mouse eggs suggests imprinting of the genome during gametogenesis. Nature **308:** 548–550.

Szabó, P., and J. R. Mann, 1994 Expression and methylation of imprinted genes during in vitro differentiation of mouse parthenogenetic and androgenetic embryonic stem cell lines. Development **120:** 1651–1660.

Szabó, P. E., and J. R. Mann, 1995 Biallelic expression of imprinted genes in the mouse germ line: implications for erasure, establishment, and mechanisms of genomic imprinting. Genes Dev. **9:** 1857–1868.

Szabó, P. E., S. H. Tang, A. Rentsendorj, G. P. Pfeifer and J. R. Mann, 2000 Maternal-specific footprints at putative CTCF sites in the H19 imprinting control region give evidence for insulator function. Curr. Biol. **10:** 607–610.

Szabó, P. E., S. H. Tang, M. R. Reed, F. J. Silva, W. M. Tsark *et al.*, 2002 The chicken β-globin insulator element conveys chromatin boundary activity but not imprinting at the mouse Igf2/H19 domain. Development **129:** 897–904.

Szabó, P. E., S. H. Tang, F. J. Silva, W. M. Tsark and J. R. Mann, 2004 Role of CTCF binding sites in the Igf2/H19 imprinting control region. Mol. Cell. Biol. **24:** 4791–4800.

Takahashi, K., T. Kobayashi and N. Kanayama, 2000 p57(Kip2) regulates the proper development of labyrinthine and spongiotrophoblasts. Mol. Hum. Reprod. **6:** 1019–1025.

Varrault, A., C. Gueydan, A. Delalbre, A. Bellmann, S. Houssami *et al.*, 2006 Zac1 regulates an imprinted gene network critically involved in the control of embryonic growth. Dev. Cell **11:** 711–722.

Westerman, B. A., A. Poutsma, L. H. Looijenga, D. Wouters, I. J. Van Wijk *et al.*, 2001 The Human Achaete Scute Homolog 2 gene contains two promotors, generating overlapping transcripts and encoding two proteins with different nuclear localization. Placenta **22:** 511–518.

Williamson, C. M., A. Blake, S. Thomas, C. V. Beechey, J. Hancock *et al.*, 2010 Mouse Imprinting Data and References. MRC Harwell, Oxfordshire. http://har.mrc.ac.uk/research/genomic_imprinting/.

Wood, A. J., and R. J. Oakey, 2006 Genomic imprinting in mammals: emerging themes and established theories. PLoS Genet. **2:** e147.

Yan, Y., J. Frisen, M. H. Lee, J. Massague and M. Barbacid, 1997 Ablation of the CDK inhibitor p57Kip2 results in increased apoptosis and delayed differentiation during mouse development. Genes Dev. **11:** 973–983.

Zhang, P., N. J. Liegeois, C. Wong, M. Finegold, H. Hou *et al.*, 1997 Altered cell differentiation and proliferation in mice lacking p57KIP2 indicates a role in Beckwith-Wiedemann syndrome. Nature **387:** 151–158.

Communicating editor: T. R. Magnuson